BULLETIN OF THE POLISH ACADEMY OF SCIENCES
TECHNICAL SCIENCES
Vol. 54, No. 4, 2006

Distribution of potential barrier height local values at Al-SiO_2 and Si-SiO_2 interfaces of the metal-oxide-semiconductor structures

K. PISKORSKI* and H.M. PRZEWLOCKI

Department of the MOS System Studies, Institute of Electron Technology, 32/46 Lotników Ave., 02-668 Warsaw, Poland

Abstract. In this work studies of barrier height local values are presented. Distribution of the gate-oxide $E_{BG}(x,y)$ and semiconductor-oxide $E_{BS}(x,y)$ barrier height local values have been determined using the photoelectric measurement methods. Two methods were used to obtain the local values of the barrier heights: modified Powell-Berglund method and modified Fowler method. Both methods were modified in such a way as to allow determination of the $E_{BG}(x,y)$ and $E_{BS}(x,y)$ distribution over the gate area using a focused UV light beam of a small diameter $d = 0.3$ mm. Measurements have been made on a series of Al-SiO_2-Si(n^+) MOS structures with semitransparent ($t_{Al} = 35$ nm) square aluminum gate (1×1 mm^2). It has been found that the $E_{BG}(x,y)$ distribution has a characteristic dome-like shape, with highest values at the center of the gate, lower at the gate edges and still lower at gate corners. On the contrary, the $E_{BS}(x,y)$ distribution is of a random character. Also, in this paper, both barrier height measurements have been compared with the photoelectric effective contact potential difference $\phi_{MS}(x,y)$ measurements. These results show good agreement between distribution of the barrier heights $E_{BG}(x,y)$ and $E_{BS}(x,y)$ measurements and independently determined shape of the effective contact potential difference $\phi_{MS}(x,y)$ distribution.

Key words: barrier height, effective contact potential difference, MOS system.

1. Introduction

It has been observed for several years in our laboratory that local values of the effective contact potential difference (ECPD or ϕ_{MS}) in Al-SiO_2-Si structures have a characteristic shape of distribution over the gate area [1,2]. An example of such a distribution shape is shown Fig. 1. In this figure the experimentally determined $V_G^0(\zeta)$ distribution is shown, where $V_G^0 = \phi_{MS} + C$ and C is a constant (see e.g. [3]). Hence, the shape of ϕ_{MS} distribution over the gate area is identical with the shape of V_G^0 distribution, shown in Fig. 1.

Mechanical stress in a MOS structure is known to influence its electrical parameters [4, 5]. One of these parameters is the effective contact potential difference ϕ_{MS}. The influence of mechanical stress on the ϕ_{MS} value of a MOS structure was quantitatively estimated [6] and it was shown that the mechanical stress has a dominating influence on the shape of the ϕ_{MS} distribution (among others by showing the influence of aluminum gate thickness on this shape). Hence, other factors which may cause non uniform distributions of ϕ_{MS} (such as non uniform distribution of electric field, due to the edge effect or to the surface roughness) are not considered in this article.

It is also known that mechanical stress is non uniformly distributed under the metal gate of a MOS structure [5, 7–9] and that it changes rapidly in the vicinity of the gate edges (Fig. 2).

Assuming, that changes in the ϕ_{MS} value are proportional to the changes in mechanical stress under the gate of the MOS structure, a model of the ϕ_{MS} distribution over the gate area was developed and verified experimentally [1,2]. A typical distribution of ϕ_{MS} local values over the square gate area, calculated using this model is shown in Fig. 3. In this figure we see the highest values in the center of the gate, lower values at the gate edges and lowest at the corners.

As shown in the next section, the ϕ_{MS} value depends directly on the difference of potential barrier heights E_{BG} and E_{BS}. Hence, one or both barrier heights must have distributions which are reflected in the ϕ_{MS} distribution over the gate area.

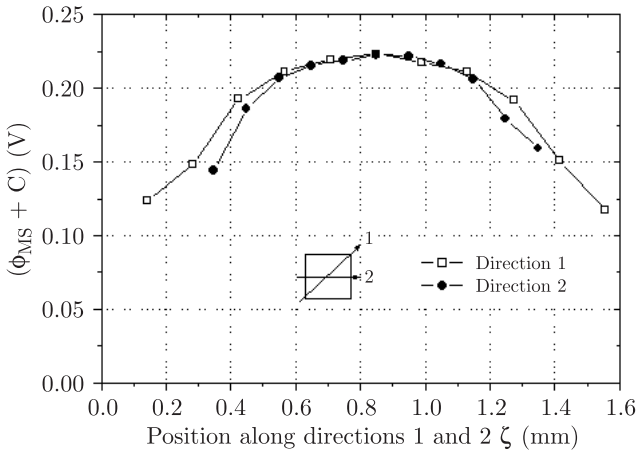

Fig. 1. Typical dependence of the $(\phi_{MS}+C)$ voltage measured at the wavelength $\lambda = 244$ nm on the position in Al-SiO_2-Si(n^+) structures with aluminum gate thickness $t_{Al} = 35$ nm and SiO_2 layer thickness $t_{OX} = 60$ nm. The direction is either (1) along the diagonal of the square gate, or (2) through the centre of the square gate and parallel to its edges

*e-mail: kpisk@ite.waw.pl

It was the purpose of this research to prove that, as expected, it is the gate-dielectric barrier height distribution $E_{BG}(x,y)$, which determines the shape of the $\phi_{MS}(x,y)$ distribution. To do this, we modified the barrier height measurements methods of Powell-Berglund and of Fowler, used these modified methods to determine distributions of both barrier heights ($E_{BG}(x,y)$, $E_{BS}(x,y)$) and compared these results with independently measured $\phi_{MS}(x,y)$ distributions.

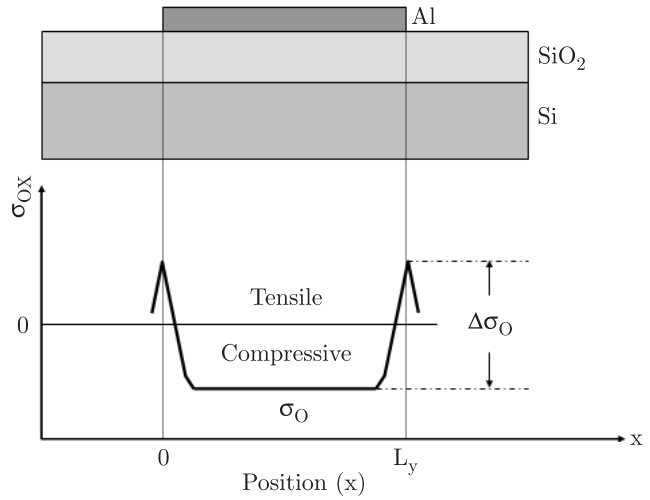

Fig. 2. The expected one-dimensional distribution of stress $\sigma_{OX}(z)$ in the oxide layer under the aluminum gate

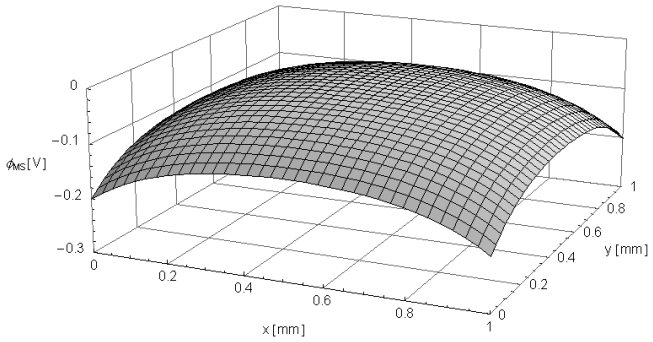

Fig. 3. Two-dimensional distribution of $\phi_{MS}(x,y)$ calculated using model after Ref. 1 for MOS structures with square gates of side length $L = 1$ mm

2. Theory

The internal photoemission phenomena may be observed in a MOS structure with a semitransparent gate, illuminated by UV radiation. The UV radiation absorbed in the electrodes (the gate or the substrate) causes excitation of some electrons. If these electrons acquire sufficient energy to surmount the potential barrier at the electrode-dielectric interface, they may pass into the insulator giving rise to a photocurrent which can be measured in the external circuit. This photocurrent I_P is a function of the barrier height E_B which electrons have to surmount, as well as of the wavelength λ of UV light illuminating the structure and the gate potential V_G. The band diagram of the MOS system is shown in Fig. 4.

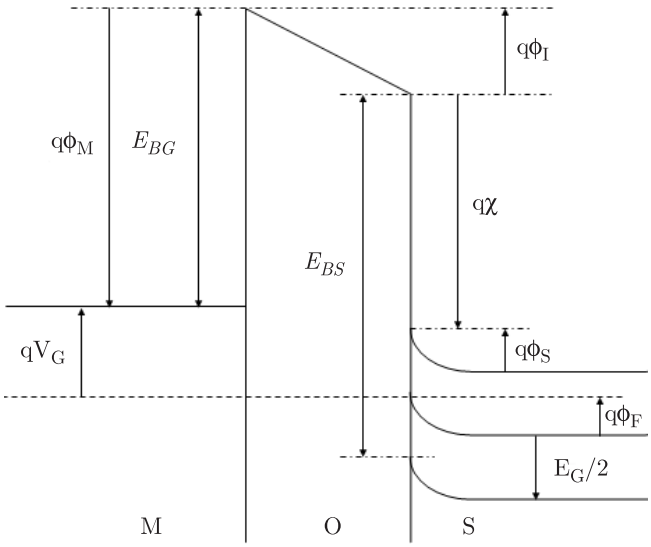

Fig. 4. Band diagram of the MOS system, at arbitrary gate potential V_G. E_{BG}, E_{BS} are potential barrier heights at gate-dielectric and semiconductor-dielectric interfaces, respectively

Balancing the potentials on both sides of the dielectric layer yields:

$$\phi_M - V_G = \chi - \phi_I - \phi_S + \frac{E_G}{2q} + \phi_F. \tag{1}$$

where: ϕ_M – the barrier height at the gate-dielectric interface, V_G – gate potential, χ – the electron affinity of the silicon substrate at the interface, ϕ_I , ϕ_S – the potential drop in the dielectric and at the semiconductor surface, $E_G/2q$ – the voltage equivalent of half energy bandgap in the semiconductor, q – the electron charge, ϕ_F – the Fermi level.

The definition of the effective contact potential difference ϕ_{MS} offers the possibility of a comparison between the difference of internal photoemission barrier heights from both sides of the dielectric and the value of ϕ_{MS}. The effective contact potential difference ϕ_{MS} is defined as [10]:

$$\phi_{MS} = \phi_M - \left(\chi + \frac{E_G}{2q} + \phi_F\right). \tag{2}$$

The value of ϕ_{MS} given by (2) depends on the doping density of the substrate (the ϕ_F value). Sometimes it is more convenient to use the value of the reduced effective contact potential difference (RECPD or ϕ^*_{MS} factor), defined as:

$$\phi^*_{MS} = \phi_M - \chi \tag{3}$$

or

$$\phi^*_{MS} = \phi_{MS} + \frac{E_G}{2q} + \phi_F. \tag{4}$$

The ϕ^*_{MS} value depends on the barrier heights on both sides of the dielectric and does not depend on the doping concentration in the substrate.

Using the band diagram shown in Fig. 4, one finds that:

$$\phi^*_{MS} = \phi_M - \chi = \frac{1}{q}\left(E_{BG} - E_{BS} + E_G\right). \tag{5}$$

Hence, using Eqs (1–4), comparisons can be made between the independently measured values of ϕ_{MS} and values of E_{BG} and E_{BS}, if the ϕ_F and E_G values are known.

The experimentally determined $I_P = f(V_G, \lambda)$ characteristics can be used to determine the individual barrier heights (E_{BG} and E_{BS}) by the well known Powell-Berglund [11–13] and Fowler [14,15] methods. An example of such $I_P = f(\lambda)$ characteristics taken for the E_{BS} barrier height determination is shown in Fig. 5.

It is well known [10], that the gate voltage V_G is a sum of three components:

$$V_G = V_I + V_S + \phi_{MS} \tag{6}$$

where: V_I – the voltage drop in dielectric and V_S – the semiconductor surface potential.

The band diagram of the MOS system for $V_G = V_{G0}$ is shown in Fig. 6. In this case the situation when voltage drop in dielectric $V_I = 0$ (flat band in dielectric) and semiconductor surface potential V_S is equal V_{S0} takes place. Hence, it results from Eq. (6) and Fig. 6 that:

$$V_{G0} = V_{S0} + \phi_{MS} \tag{7}$$

where: V_{S0} – the semiconductor surface potential for $V_G = V_{G0}$.

Measuring $I_P = f(V_G)$ characteristics for different (values (Fig. 7) and choosing the one which is symmetrical with respect to the $I_P = 0$ point, the value of gate voltage $V_G = V_{G0}$, at which $V_I = 0$ can be determined [3]. This can be done with an accuracy of the order of ± 1 mV [16].

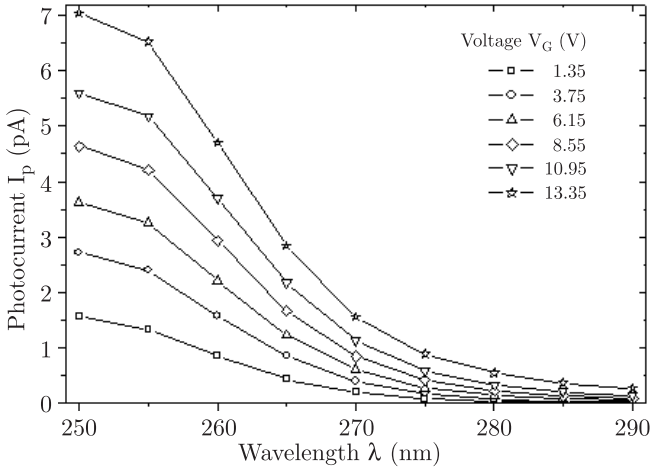

Fig. 5. Typical spectral characteristics $I_P = f(\lambda)$ for the EBS barrier height measurements

Having found V_{G0}, one still has to find V_{S0}, to determine ϕ_{MS} from Eq. (7). V_{S0} can be determined in a separate measurement (e.g. from the value of the MOS capacitance C at $V_G = V_{G0}$), or it can be made negligible in comparison with ϕ_{MS} (e.g. by using heavily doped substrate MOS structures). These two approaches allow the determination of ϕ_{MS}, with ± 10 mV accuracy, or better [3].

The principle of the recently developed modification of the photoelectric E_{BG} and E_{BS} measurement method is illustrated in Fig. 8.

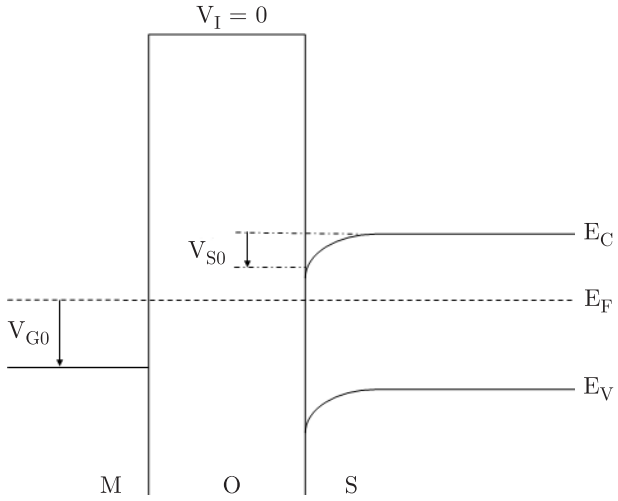

Fig. 6. Band diagram of MOS structure at $V_G = V_{G0}$

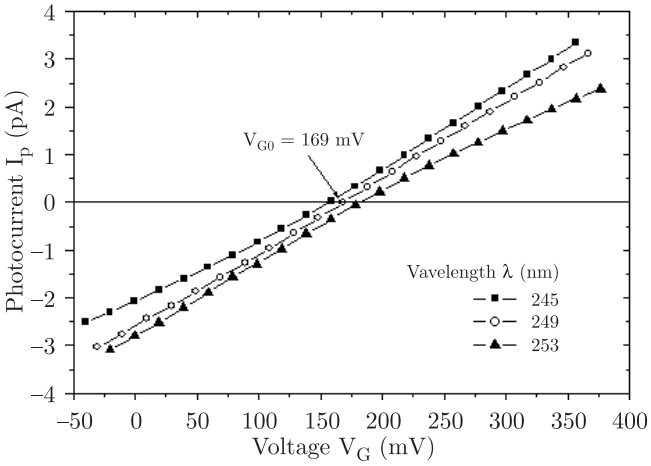

Fig. 7. The experimental characteristics $I_P = f(V_G)$ taken for the V_{G0} voltage determination

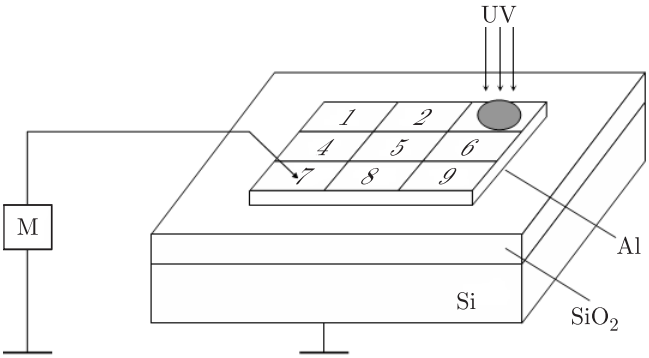

Fig. 8. The measurement system: the MOS structure with semitransparent Al gate is illuminated in 9 different locations over the gate area by a focused light beam. The photocurrent is measured in the external circuit M

Barrier heights were measured by both methods: modified Powell-Berglund method and modified Fowler method. The modifications of both methods consisted in using a UV light

beam of a relatively small diameter $d = 0.3$ mm in comparison with the side length of a square Al gate. A focused light beam illuminates a small fragment of the gate area (9 different locations in this case), causing internal photoemission to take place in this region of the MOS structure. Hence, it was possible to measure local values of both gate-dielectric E_{BG} and dielectric-semiconductor E_{BS} barrier heights. Scanning the gate with the UV light beam allows determination of the lateral E_{BG} and E_{BS} distribution over the gate area.

The principle of the V_{G0} local value measurement is as described in relation to Fig. 7. The resulting photocurrent I_P vs. gate voltage V_G characteristics (for example Fig. 7) can be taken in the external circuit M (Fig. 8). Analysis of these characteristics allows determination of the local V_{G0} values in the illuminated region.

3. Experimental details

In this work measurements were made on Al-SiO_2-Si capacitors with semitransparent ($t_{\mathrm{Al}} = 35$ nm) square (1×1 mm^2) gate. Phosphorus doped n^+ substrates ($\rho = 0.015$ Ωcm) of <100> orientation were used to simplify interpretation of the photoelectric measurements, as discussed in [1,3]. Wafers were thermally oxidized at temperature $T = 1000$°C, in dry oxygen, to grow a SiO_2 layer of thickness $t_{OX} = 60$ nm. Although SiO_2 layers of current technological interest are thinner than $t_{OX} = 3$ nm, we used thicker oxides to optimize the sensitivity of the applied photoelectric methods.

Oxidized wafers were subsequently annealed in nitrogen for $t = 10$ min and $t = 120$ min, at $T = 1050$°C. The post metalization annealing was carried out for $t = 20$ min, at $T = 450$°C in forming gas atmosphere. Photoelectric measurements of barrier heights were made after all the structures were checked for gross defects, such as non negligible leakage currents, ionic instability, low breakdown voltage of the SiO_2 layer, etc., and the defective structures were eliminated.

The absolute accuracy of E_{BG} and E_{BS} determination is estimated to be ± 50 meV. However, the relative accuracy in determining the changes of E_{BG} and E_{BS} in consecutive measurements (in different places over the gate area) is better and is estimated to be ± 10 meV.

4. Results and discussion

Measurements of local E_{BG} and E_{BS} barrier heights were made by both modified Powell-Berglund and (for comparison) by the modified Fowler method, in nine locations over the gate area (as shown in Fig. 8), on each of the 26 MOS structures on one silicon wafer.

The so determined values were averaged in such a way that average local E_{BG} and E_{BS} values were determined for each of the nine positions over the gate area and then were connected by smooth (3rd order polynomial) lines to obtain approximate distributions of barrier heights over the entire gate area of the MOS structure.

Such distributions of the averaged values are shown in Figs. 9a and 9b for measurements made by the modified Powell-Berglund method and in Figs. 10a and 10b for measurements made by the modified Fowler method.

Figure 9a and 10a show that averaged $E_{BG}(x, y)$ distribution has a dome-like shape and the difference between maximum $E_{BG\,\max}$ and minimum $E_{BG\,\min}$ local barrier height values over the gate area, ($E_{BG\,\max} - E_{BG\,\min}$) remains relatively large (68 or 45 meV) in comparison with averaged $E_{BS}(x, y)$ distribution, shown in Fig. 9b and 10b, which has a random character and a smaller $E_{BS\,\max} - E_{BS\,\min}$ difference (18 or 10 meV). Moreover, this difference shows a decreasing tendency with the increasing number of MOS structures measured and taken into account in the averaging process.

The $E_{BG\,\max} - E_{BG\,\min}$ difference is called the amplitude of the E_{BG} distribution, similarly $E_{BS\,\max} - E_{BS\,\min}$ is called the amplitude of the E_{BS} distribution. It is clearly seen that the amplitude of E_{BG} distribution is c.a. 4 times larger than the amplitude of the E_{BS} distribution.

$$\frac{E_{BG\,\max} - E_{BG\,\min}}{E_{BS\,\max} - E_{BS\,\min}} \cong 4 \tag{8}$$

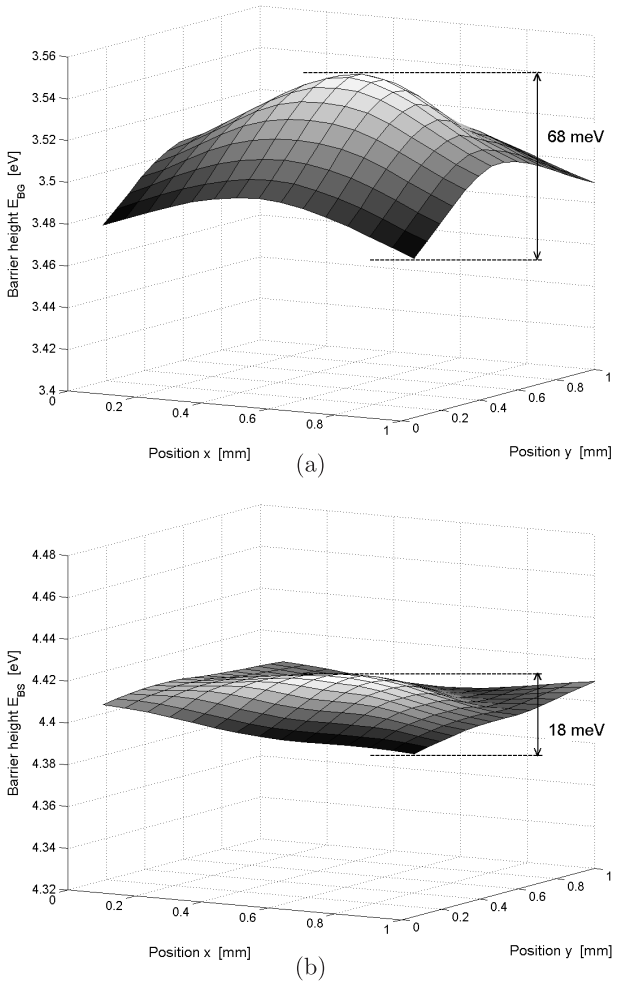

Fig. 9. Averaged two-dimensional distribution of a) E_{BG} and b) E_{BS} barrier heights measured using modified Powell-Berglund method for 26 MOS structures. Average E_{BG} and E_{BS} values were found for each of the 9 locations over the gate area (shown in Fig. 8) and used to determine distributions shown in the figure

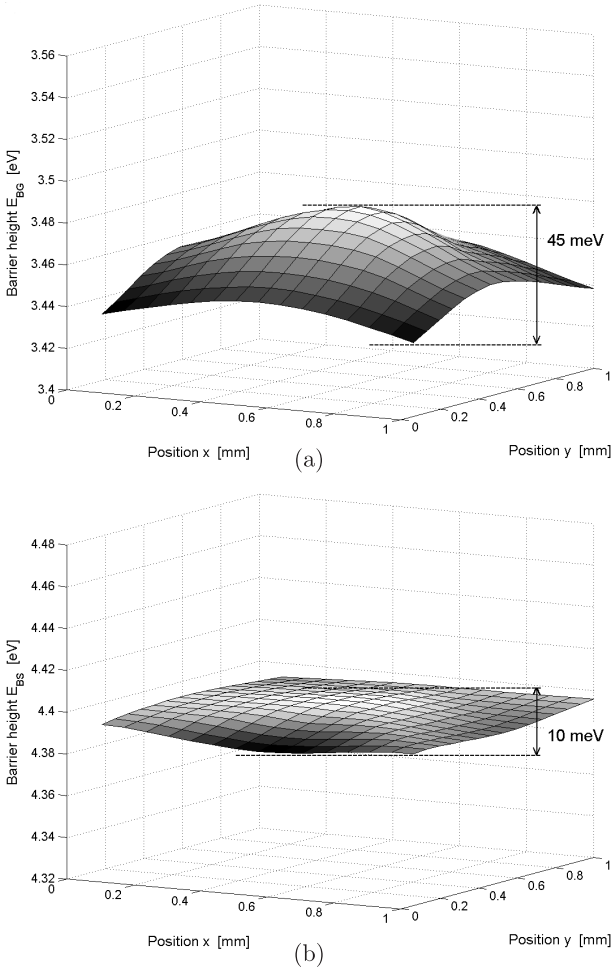

Fig. 10. Averaged two-dimensional distribution of a) E_{BG} and b) E_{BS} barrier heights measured using modified Fowler method for 26 MOS structures. Average E_{BG} and E_{BS} values were found for each of the 9 locations over the gate area (shown in Fig. 8) and used to determine distributions shown in the figure

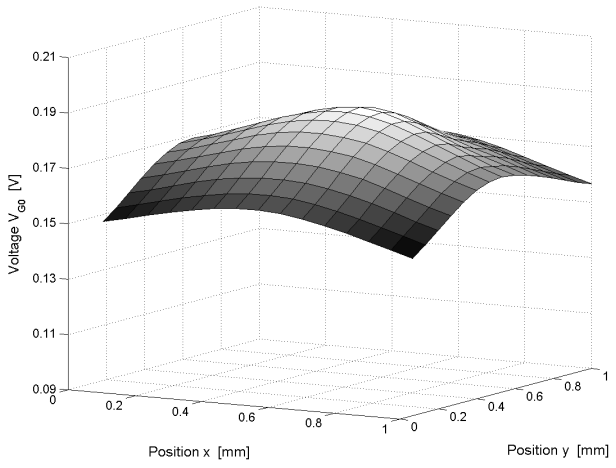

Fig. 11. Averaged two-dimensional distribution of V_{G0} values measured for 26 MOS structures. Average V_{G0} values were found for each of the 9 locations over the gate area (shown in Fig. 8) and used to determine the distribution shown in the figure

There are slight differences between averaged distributions obtained by both measurement methods (compare Fig. 9a with Fig. 10a, and Fig. 9b with 10b), which are due to measurement inaccuracies by both methods, but the general features of averaged $E_{BG}(x,y)$ and $E_{BS}(x,y)$ distributions do not depend on the measurement method applied.

On the other hand, the V_{G0} voltage ($V_{G0} \cong \phi_{MS}$ in this case) also has a characteristic dome-like shape of distribution over the gate area with local V_{G0} values being highest in the middle of the gate, lower at the gate edges, and lowest at gate corners. Fig. 11 shows the measured and averaged $V_{G0}(x,y)$ distribution over the gate area.

To simplify explanation of the obtained results we propose the following symbols for the ϕ^*_{MS} (or RECPD) value:

– $\phi^*_{MS}(1)$ – the reduced effective contact potential difference determined applying Eq. (4) in which ϕ_{MS} values measured by the photoelectric method [3] are used,
– $\phi^*_{MS}(2)$ – the reduced effective contact potential difference calculated (Eq. 5) using the E_{BG} and E_{BS} values measured by both modified Powell-Berglund and modified Fowler methods.

Subtracting Eq. (3) from Eq. (4) we have:

$$\phi^*_{MS}(1) - \phi^*_{MS}(2) = \phi_{MS} - \phi_M + \chi + \frac{E_G}{2q} + \phi_F = R. \quad (9)$$

The R factor should be equal to 0 for ideally accurate measurements. Otherwise we consider R to stand for the error of the barrier height measurement (since we know that ϕ_{MS} is measured much more accurately [3,9]). The value of R higher than 10 mV means that at least one of the considered barrier heights was measured inaccurately.

The averaged $\phi^*_{MS}(1)(x,y)$ distribution over the gate area is similar to the $V_{G0} \cong \phi_{MS}$ distribution shown in Fig. 11, just shifted vertically according to Eq. (4).

Figure 12 shows averaged $\phi^*_{MS}(2)(x,y)$ distribution for the modified Powell-Berglund method (Fig. 12a) and for the modified Fowler method (Fig. 12b) over the gate area.

In Fig. 12 characteristic dome-like shape of the $\phi^*_{MS}(2)(x,y)$ distribution over the gate area for both measurement methods can be observed. There are slight differences between $\phi^*_{MS}(2)$ distributions determined by modified Powell-Berglund and by modified Fowler method, as can be seen in Fig. 12a and 12b. These differences are due to the inaccuracies of both barrier height measurement methods.

The differences between $\phi^*_{MS}(1)$ and $\phi^*_{MS}(2)$ values (calculated by Eq. (9)) for the modified Powell-Berglund method and modified Fowler method on each position over the gate area are given in Table 1.

Table 1
Values of the measurement error R

Positions over the gate area	1	2	3	4	5	6	7	8	9
Powell-Berglund R [mV]	20	1	9	13	–2	1	15	1	18
Fowler R[mV]	49	39	45	51	44	47	53	51	55

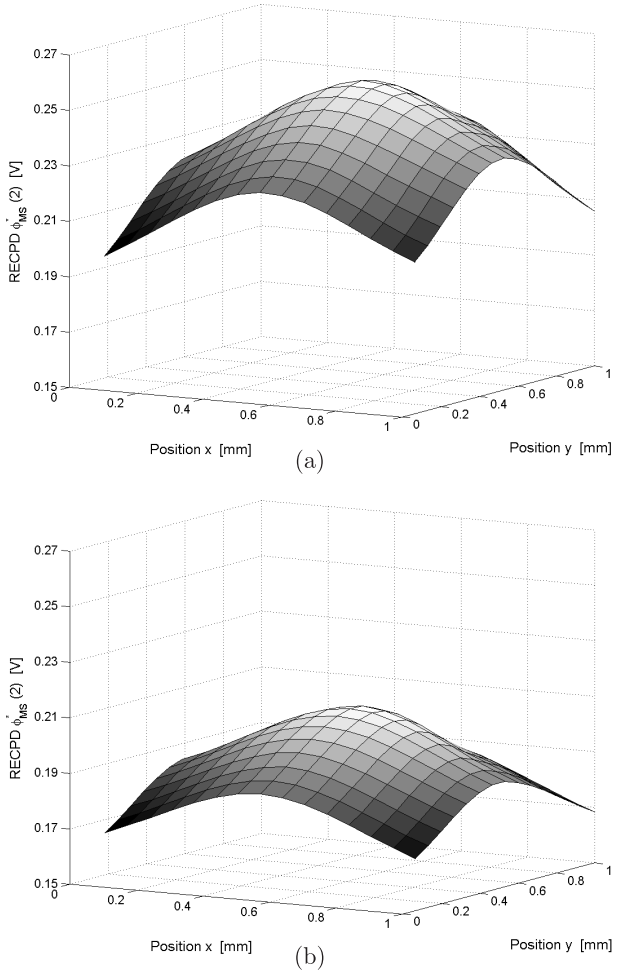

Fig. 12. Averaged two-dimensional distribution of $\phi^*_{MS}(2)$ reduced effective contact potential difference calculated using E_{BG} and E_{BS} values determined by: a) the modified Powell-Berglund method and b) the modified Fowler method for 26 MOS structures. Average $\phi^*_{MS}(2)$ values were found for each of the 9 locations over the gate area (shown in Fig. 8) and used to determine distributions shown in the figure

The positive value of the measurement error R may be explained by too low a value of the E_{BG} barrier height or too high a value of the E_{BS} barrier height. The opposite applies when $R < 0$.

Good agreement between the $\phi^*_{MS}(1)(x, y)$ and $\phi^*_{MS}(2)(x, y)$ values has been observed for measurements made by modified Powell-Berglund method ($R_{\max} = 20$ mV at gate corner – position 1, $R_{\min} = 1$ mV at gate edges – position 6). The modified Fowler method compares unfavourably with the modified Powell-Berglund method. The values of error R for each of the nine positions over the gate area (about 40–50 mV) are much higher than respective values for the modified Powell-Berglund method. Hence, it is clearly seen that the complexity of the modified Fowler method is not balanced by higher measurement accuracy, while the simple modified Powell-Berglund method yields relatively accurate measurement results.

In Table 2 are given the average values of R (in [mV]) for analogous positions over the gate area.

Table 2
The average values of R (in [mV]) for analogous positions over the gate area

Positions over gate area	Powell-Berglund	Fowler
1,3,7,9 (corners)	15.5	50.5
2,4,6,8 (edges)	4	47
5 (center)	–2	44

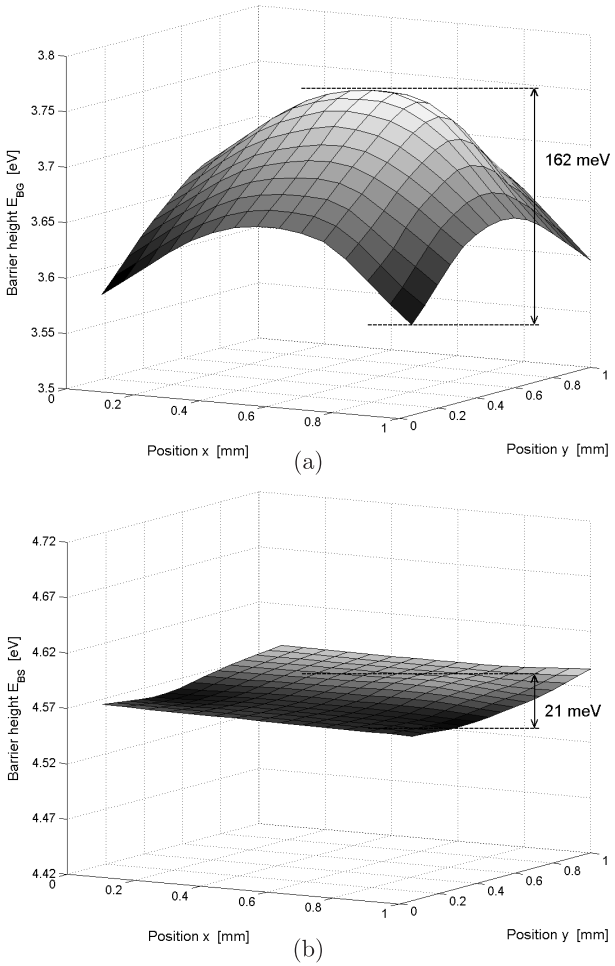

Fig. 13. Averaged two-dimensional distribution of (a) E_{BG} and (b) E_{BS} barrier heights measured using modified Powell-Berglund method for 30 MOS structures. Average E_{BG} and E_{BS} values were found for each of the 16 locations over the gate area and used to determine distributions shown in the figure

In case of the measurements made by both methods the highest values of R at gate corners, lower values at gate edges and lowest value at the center of the gate can be observed.

To confirm the results reported above, a similar investigation was made using the UV light beam of a smaller diameter $d = 0.25$ mm. This allowed to find local barrier heights values in 16 different positions over the gate area (instead of 9 positions, as shown in Fig. 8). Measurements were made on 30 MOS structures, on one silicon wafer (which, however, was differently processed than the wafer used in previously described measurements) and the averaging procedure was the same as described above.

The differences between results obtained by two methods were found to be insignificant in this case, hence, the results of measurements made by modified Fowler method won't be discussed here.

Results of the E_{BG} and E_{BS} distributions obtained in this case are shown in Fig. 13. These results fully confirm the dome-like shape of the E_{BG} distribution and the essentially uniform distribution of E_{BS} over the gate area. The more pronounced dome-like shape of the E_{BG} distribution shown in Fig. 13a, as compared to the distribution shown in Fig. 9a is due to different processing of the samples used in the measurements.

The scatter of measurement results obtained in practice is illustrated in Fig. 14. In this figure average values of local barrier heights in different positions over the gate area are shown (connected by straight lines), together with standard deviations of results (shown by error bars).

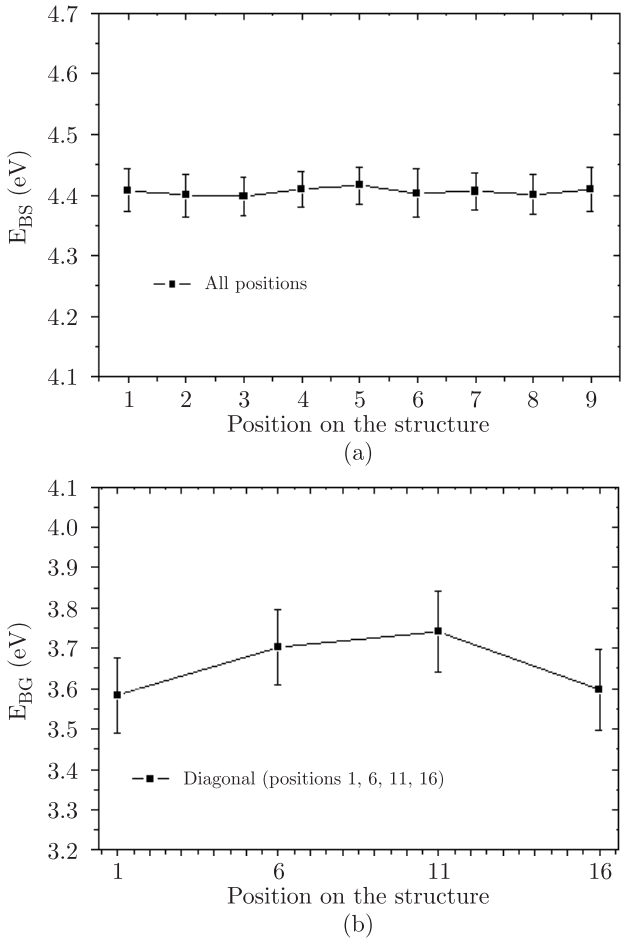

Fig. 14. Average values, shown by points connected by straight lines and standard deviations, shown by error bars, of local barrier height measurement results. a) Local E_{BS} measurement results for all the nine positions in the 3×3 matrix over the gate area. b) Local E_{BG} measurement results in four positions lying on the diagonal of the 4×4 matrix over the gate area

5. Conclusions

The lateral distribution of local E_{BG} and E_{BS} barrier height values over the gate area of a MOS structure were studied. Measurements were made on two series of 26 and 30 Al-SiO_2-Si(n^+) capacitors. Two photoelectric measurement methods were used in this investigation: modified Powell-Berglund method and modified Fowler method. The modifications of these methods consisted in applying a focused UV light beam (diameter $d = 0.3$ and 0.25 mm) which allowed measurements to be made in 9 and 16 different locations over the gate area. It was found that E_{BG} barrier height has a characteristic dome-like shape of distribution, with highest values in the middle of the gate, lower at gate edges, and lowest at gate corners. On the other hand, the E_{BS} barrier height distribution has a random character and differences between highest and lowest values of E_{BS} (so-called amplitude) for any of the measured MOS structures are much smaller than the respective differences in E_{BG} values.

The dome-like shape of $E_{BG}(x, y)$ distribution is identical with the shape of independently (and much more accurately) measured distributions of $\phi_{MS}(x, y)$ over the gate area. This proves that, as expected, the shape of the ϕ_{MS} distribution results directly from the distribution of gate-dielectric barrier height $E_{BG}(x, y)$ over the gate area. We ascribe the dome-like shape of the E_{BG} distribution to the non uniform distribution of mechanical stress at the gate-dielectric interface in a MOS structure.

References

[1] H.M. Przewlocki, A. Kudla, D. Brzezinska, and H.Z. Massoud, "Distribution of the contact-potential difference local values over the gate area of MOS structures", *Microelectronic Engineering* 72, 165–173 (2004).

[2] A. Kudla, H.M. Przewlocki, L. Borowicz, D. Brzezinska, and W. Rzodkiewicz, "Photoelectrical measurements of the local value of the contact-potential difference in metal-insulator-semiconductor (MIS) structures", *Thin Solid Films* 450, 203–206 (2004).

[3] H.M. Przewlocki, "Theory and applications of internal photoemission in the MOS system at low electric fields", *Sol. State Electronics* 45, 1241–1250 (2001).

[4] C.H. Bjorkman, J.T. Fitch, and G. Lucovsky, "Correlation between midgap interface state density and thickness-averaged oxide stress and strain at Si/SiO_2 interfaces formed by thermal oxidation of Si", *Appl. Phys. Lett.* 56 (20), 1983–1985 (1990).

[5] S.M. Hu, "Stress-related problems in silicon technology", *J. Appl. Phys.* 70 (6), R53-R80 (1991).

[6] H.M. Przewlocki and H.Z. Massoud, "The effects of stress annealing in nitrogen on the effective contact-potential difference, charges, and traps at the Si/SiO_2 interface of metal-oxide-semiconductor devices", *J. Appl. Phys.* 92 (4), 2198–2201 (2002).

[7] I. De Wolf, H. E. Maes, and S. K. Jones, "Stress measurements in silicon devices through Raman spectroscopy: bridging the gap between theory and experiment", *J. Appl. Phys.* 79 (9), 7148–7156 (1996).

[8] K.F. Dombrowski, I. de Wolf, and B. Dietrich, "Stress measurements using ultraviolet micro-Raman spectroscopy", *J. Appl. Phys.* 75 (16), 2450–2451 (1999).

[9] A. Kudla, "Fotoelectric methods for determining the height of potential barriers in the MOS structure", *Works of the Institute of Electron Technology* 5–7, 7–115 (1998), (in Polish).

[10] E.H. Nicollian and J.R. Brews, *MOS (Metal Oxide Semiconductor) Physics and Technology*, John Wiley & Sons, New York, 1982.

[11] R.J. Powell and C.N. Berglund, "Photoinjection into SiO2: use of optical interference to determine electron and hole contribution", *J. Appl. Phys.* 40, 5093–5101 (1969).

[12] R. J. Powell, "Interface barrier energy determination from voltage dependence of photoinjected currents", *J. Appl. Phys.* 41, 2424–2432 (1970).

[13] R. J. Powell and C. N. Berglund, "Photoinjection studies of charge distributions in oxides of MOS structures", *J. Appl. Phys.* 42, 4390–4397 (1971).

[14] H. Fowler, "The analysis of photoelectric sensitivity curves for clean metals at various temperatures", *Phys. Rev.* 38, 45–56 (1931).

[15] V. Afanase'ev and V.K. Adamchuk, "Internal photoemission spectroscopy of semiconductor-insulator interfaces", *Progress in Surface Sci.* 41, 111 (1992).

[16] H.M. Przewlocki, "Internal photoemission in the MOS system at low electric fields in the dielectric. Model and application", *Microel. Reliab.* 40 (4–5), 581–584 (2000).